

Entanglement of two distinguishable atoms in a rectangular waveguide: Linear approximation with single excitation

Jing Li(李静), Lijuan Hu(胡丽娟), Jing Lu(卢竞), and Lan Zhou(周兰)
Citation: Chin. Phys. B, 2021, 30 (**9**): 090307. DOI: 10.1088/1674-1056/ac0bb3
Journal homepage: http://cpb.iphy.ac.cn; http://iopscience.iop.org/cpb

What follows is a list of articles you may be interested in

Nonlocal advantage of quantum coherence and entanglement of two spins under intrinsic decoherence

Bao-Min Li(李保民), Ming-Liang Hu(胡明亮), and Heng Fan(范桁)
Chin. Phys. B, 2021, 30 (**7**): 070307. DOI: 10.1088/1674-1056/abff2a

Steered coherence and entanglement in the Heisenberg *XX* chain under twisted boundary conditions

Yu-Hang Sun(孙宇航) and Yu-Xia Xie(谢玉霞)
Chin. Phys. B, 2021, 30 (**7**): 070303. DOI: 10.1088/1674-1056/abe1a9

Continuous-variable quantum key distribution based on photon addition operation

Xiao-Ting Chen(陈小婷), Lu-Ping Zhang(张露萍), Shou-Kang Chang(常守康), Huan Zhang(张欢), and Li-Yun Hu(胡利云)
Chin. Phys. B, 2021, 30 (**6**): 060304. DOI: 10.1088/1674-1056/abd931

Entanglement properties of GHZ and W superposition state and its decayed states

Xin-Feng Jin(金鑫锋), Li-Zhen Jiang(蒋丽珍), and Xiao-Yu Chen(陈小余)
Chin. Phys. B, 2021, 30 (**6**): 060301. DOI: 10.1088/1674-1056/abd74e

Deterministic nondestructive state analysis for polarization-spatial-time-bin hyperentanglement with cross-Kerr nonlinearity

Hui-Rong Zhang(张辉荣), Peng Wang(王鹏), Chang-Qi Yu(于长琦), and Bao-Cang Ren(任宝藏)
Chin. Phys. B, 2021, 30 (**3**): 030304. DOI: 10.1088/1674-1056/abd7d5

Entanglement of two distinguishable atoms in a rectangular waveguide: Linear approximation with single excitation*

Jing Li(李静)[1], Lijuan Hu(胡丽娟)[2], Jing Lu(卢竞)[1], and Lan Zhou(周兰)[1,2,†]

[1] *Affiliation Synergetic Innovation Center for Quantum Effects and Applications, Key Laboratory for Matter Microstructure and Function of Hunan Province, Key Laboratory of Low-Dimensional Quantum Structures and Quantum Control of the Ministry of Education, School of Physics and Electronics, Hunan Normal University, Changsha* 410081, *China*

[2] *College of Science, Hunan University of Science and Engineering, Yongzhou* 425199, *China*

(Received 8 April 2021; revised manuscript received 22 May 2021; accepted manuscript online 17 June 2021)

We investigate the entanglement dynamics of two distinguishable two-level systems (TLSs) characterized by energy difference δ located inside a rectangular hollow metallic waveguide of transverse dimensions a and b. The effects of energy difference δ and the inter-TLS distance on the time evolution of the concurrence of the TLSs are examined in the single excitation subspace when the energy separation of the TLS is far away from the cutoff frequencies of the transverse mode.

Keywords: entanglement, concurrence, two two-level systems, energy separations

PACS: 03.65.Yz, 03.65.–w **DOI:** 10.1088/1674-1056/ac0bb3

1. Introduction

The principle of quantum superposition allows a system to be composed of multiple quantum systems that cannot be decomposed into the product of individual quantum states. This nonseparability, labeled as entanglement, is an important physical resource for applications of quantum information processing. Quantum network is essentially based on a scalable quantum information processing.[1] A quantum network consists of quantum channels and nodes. Two-level systems (TLSs) fixed at quantum nodes are called stationary qubits which generate, store, and process quantum information. It is essentially important to generate or keep the correlation among TLSs located at different positions for protecting quantum information. The bipartite entanglement involving two TLSs is of special interest. Spatially separated TLSs' talking to each other can be either mediated or destroyed via electromagnetic fields.[2–6] Complete disentanglement is achieved in finite time for two TLSs coupled individually to two vacuum cavities.[7,8] The entanglement exhibits revivals in time for two TLSs coupled collectively to a multimode vacuum field in free space.[9,10]

To build large scale quantum networks, an electromagnetic field in a one-dimensional (1D) waveguide is of special interest. The electromagnetic field is confined spatially in two dimensions and propagates along the remaining one, so it consists of infinite modes for right and left-going photons of continuous varying frequencies. Spontaneously emitted waves from the TLS will interfere with the incident wave.[11–26] The coupling of the electromagnetic field to a TLS can be increased by reducing the transverse size. A waveguide with a cross section has many guiding modes, *e.g.*, transverse-magnetic (TM) modes or transverse-electric (TE) ones. However, most work only consider TLSs interacting with one guiding mode of the waveguide,[14–33] which means that the transverse-size effect has been ignored. In this paper, we study the time evolution of entanglement measure for two uncoupled TLSs interacting with the electromagnetic field confined in a 1D rectangular hollow metallic waveguide. The TLSs share initially an excitation and the field is in vacuum. Such waveguide has many guiding modes. There is a continuous range of frequencies and a minimum frequency (called cutoff frequency) allowed in each guiding mode.[34] When the transitions of the TLSs are far away from the cutoff frequencies of guiding modes, the probability amplitudes of the TLSs is described by the delay differential equations by tracing out the continuum of bosonic modes in the waveguide. The influence on the time evolution of the concurrence of the TLSs are examined by inspecting the following identities: the difference of TLSs' energy separations characterized by δ, the inter-TLS distance d, and the number of the guiding modes.

This paper is organized as follows. In Section 2, we introduce the model and establish the notation. In Section 3, we derive the relevant equations describing the dynamics of the system for the case of the TLSs being initially sharing an excitation and the waveguide mode in the vacuum state. In Section 4, we analyze the behavior of the TLSs' concurrence when the TLSs interact resonantly with the electromagnetic field of one or two guiding modes. We make a conclusion in Section 5.

*Project supported by the National Natural Science Foundation of China (Grant Nos. 11975095, 12075082, and 11935006), the Science and Technology Innovation Program of Hunan Province, China (Grant No. 2020RC4047), and the Construct Program of Applied Characteristic Discipline in Hunan University of Science and Engineering.

†Corresponding author. E-mail: zhoulan@hunnu.edu.cn

© 2021 Chinese Physical Society and IOP Publishing Ltd

2. Two TLSs in a rectangular waveguide

The Hamiltonian of the TLSs interacting with the electromagnetic field of a rectangular waveguide consist of three parts

$$\hat{H} = \hat{H}_{\rm a} + \hat{H}_{\rm f} + \hat{H}_{\rm int}. \tag{1}$$

The fist part is the free Hamiltonian of the TLSs

$$\hat{H}_{\rm a} = \sum_{l=1}^{2} \hbar\omega_l \hat{S}_l^{+}\hat{S}_l^{-}, \tag{2}$$

where $\hat{S}_l^{+} \equiv |e_l\rangle\langle g_l|$ ($\hat{S}_l^{-} \equiv |g_l\rangle\langle e_l|$) is the rising (lowing) atomic operator of the l-th TLS, ω_l ($l = 1,2$) is the energy difference between the excited state $|e\rangle$ and the ground state $|g\rangle$.

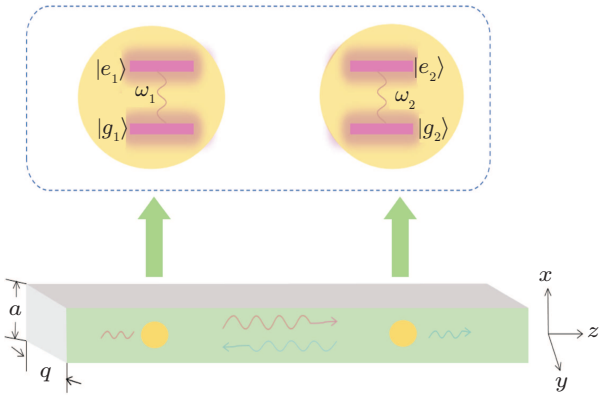


Fig. 1. Schematic illustration for an infinite waveguide of rectangular cross section $A = aq$ (a) coupling to two TLSs, (b) located at $\boldsymbol{r}_1 = (a/2, q/2, z)$ and $\boldsymbol{r}_2 = (a/2, q/2, z+d)$.

The rectangular hollow metallic waveguide made of perfect conductors is confined in the x–y plane with the area $A = aq$ of its cross section, and translational invariant in the z direction, as shown in Fig. 1. For the convenience of later discussion, we set $a = 2q$. The fields in the rectangular waveguide are classified as transverse magnetic (TM) or transverse electric (TE) according to whether the electric field or magnetic field is transverse to the axial direction of the guide. Each guiding mode is characterized by three wave numbers $\{m\pi/a, n\pi/q, k\}$. Its dispersion relation is given by $\omega_{(m,n,k)} = \sqrt{\Omega_{(m,n)}^2 + (ck)^2}$, where $\Omega_{(m,n)} = c\sqrt{(m\pi/a)^2 + (n\pi/q)^2}$ is the cutoff frequency. We note that we only study the role of the guiding modes in this paper and the evanescent modes are not considered. The free Hamiltonian of the fields reads

$$\hat{H}_{\rm f} = \sum_j \int {\rm d}k \hbar\omega_{jk} \hat{a}_{jk}^{\dagger}\hat{a}_{jk}, \tag{3}$$

where $\hat{a}_{jk}^{\dagger}$ ($\hat{a}_{jk}$) is the creation (annihilation) operator of the ${\rm TM}_{(m,n)}$ modes. Here, the numbers (m,n) have been replaced with the sequence number j, *i.e.*, $j = 1,2,3,\ldots$. The reason why only ${\rm TM}_{(m,n)}$ modes are considered will be given in the following. Two TLSs, named TLS 1 and TLS 2, are separately located inside the waveguide at positions $\boldsymbol{r}_1 = (a/2, q/2, z_1)$ and $\boldsymbol{r}_2 = (a/2, q/2, z_2)$, the distance between the TLSs is denoted by $d = z_2 - z_1$. We assume the dipoles of TLSs are along the z axis. In this case, only the ${\rm TM}_{(m,n)}$ guiding modes with odd integer m and n are interact with the TLSs. The interaction between the TLSs and the electromagnetic field is written as

$$\hat{H}_{\rm int} = \sum_{l=1}^{2}\sum_j \int {\rm d}k \frac{{\rm i}g_{jl}\hbar}{\sqrt{\omega_{jk}}} {\rm e}^{{\rm i}kz_l} \hat{S}_l^{-}\hat{a}_{jk}^{\dagger} + {\rm h.c.}, \tag{4}$$

in the electric dipole and rotating wave approximations, where

$$g_{jl} = \Omega_j \mu_l \times \sin\left(\frac{m\pi}{2}\right)\sin\left(\frac{n\pi}{2}\right)/\sqrt{A\hbar\pi\varepsilon_0}$$

and μ_l is the magnitude of the dipole of the l-th TLS. We assume that μ_l is real. If the dipoles $\mu_l = \mu$, the parameter g_{jl} is independent of the subscript l and it becomes

$$g_j = \frac{\Omega_{(m,n)}\mu}{\sqrt{\hbar A\pi\varepsilon_0}} \sin\left(\frac{m\pi}{2}\right)\sin\left(\frac{n\pi}{2}\right), \tag{5}$$

where ε_0 is the permittivity of free space, and $j = (1,1),(3,1),(5,1),\ldots$ in the ascending order.

3. Time evolution of the TLSs

In the case of a single excitation present in the system, the state vector of the system can be written as

$$|\psi(t)\rangle = b_1|eg0\rangle + b_2|ge0\rangle + \sum_j \int {\rm d}k b_{jk}\hat{a}_{jk}^{\dagger}|gg0\rangle, \tag{6}$$

where $|0\rangle$ is the vacuum state of the quantum field, $b_l(t)$, $l = 1,2$ is the probability amplitude for TLS l being excited, $b_{jk}(t)$ is the probability amplitude for the excitation in a mode k of the ${\rm TM}_j$ guiding mode. The initial state of the system is denoted by the amplitudes $b_{jk}(0) = 0$, $b_1(0)$, $b_2(0)$. The Schrödinger equation results in the following coupled equation of the amplitudes:

$$\dot{b}_1 = -{\rm i}\omega_1 b_1 - \sum_j \int {\rm d}k b_{jk}\frac{g_{j1}}{\sqrt{\omega_{jk}}}{\rm e}^{-{\rm i}kz_1}, \tag{7a}$$

$$\dot{b}_2 = -{\rm i}\omega_2 b_2 - \sum_j \int {\rm d}k b_{jk}\frac{g_{j2}}{\sqrt{\omega_{jk}}}{\rm e}^{-{\rm i}kz_2}, \tag{7b}$$

$$\dot{b}_{jk} = -{\rm i}\omega_{jk} b_{jk} + \frac{{\rm e}^{{\rm i}kz_1}}{\sqrt{\omega_{jk}}}\left(g_{j1}b_1 + g_{j2}b_2{\rm e}^{{\rm i}kd}\right). \tag{7c}$$

We introduce three new variables to remove the high-frequency effect

$$b_1(t) = B_1(t){\rm e}^{-{\rm i}\omega_{\rm A}t}, \tag{8a}$$

$$b_2(t) = B_2(t){\rm e}^{-{\rm i}\omega_{\rm A}t}, \tag{8b}$$

$$b_{jk}(t) = B_{jk}(t){\rm e}^{-{\rm i}\omega_{jk}t}, \tag{8c}$$

and define the mean frequency of the TLSs as well as the difference of the TLSs' frequencies

$$\omega_{\rm A} = \frac{\omega_2 + \omega_1}{2}, \quad \delta = \frac{\omega_1 - \omega_2}{2}. \tag{9}$$

Then, we formally integrate equation of $B_{jk}(t)$, which is later inserted into the equations for $B_1(t)$, and $B_2(t)$. The probability amplitudes for one TLS being excited are determined by two coupled integro-differential equations. Assuming that the frequency $\omega_{\rm A}$ is far away from the cutoff frequencies Ω_j, we can expand ω_{jk} around $\omega_{\rm A}$ up to the linear term

$$\omega_{jk} = \omega_{\rm A} + v_j\left(k - k_{j0}\right), \tag{10}$$

where the wavelength of the emitted radiation $k_{j0} = \sqrt{\omega_{\rm A}^2 - \Omega_j^2}/c$ is determined by $\omega_{jk_0} = \omega_{\rm A}$, and the group velocity

$$v_j \equiv \frac{{\rm d}\omega_{jk}}{{\rm d}k}\Big|_{k=k_{j0}} = \frac{c\sqrt{\omega_{\rm A}^2 - \Omega_j^2}}{\omega_{\rm A}}, \tag{11}$$

is different for different ${\rm TM}_j$ guiding modes. Integrating over all wave vectors k gives rise to a linear combination of $\delta(t-\tau-\tau_j)$ and $\delta(t-\tau)$, where $\tau_j = d/v_j$ is the delay time that the emitted photon travels from one TLS to the other TLS in the given transverse mode j. The dynamics of two TLSs is governed by the differential equations[35–39]

$$(\partial_t + \Gamma_1 + {\rm i}\delta)B_1(t) = -\sum_j \gamma_j {\rm e}^{{\rm i}\varphi_j} B_2(t_j)\Theta(t_j), \tag{12a}$$

$$(\partial_t + \Gamma_2 - {\rm i}\delta)B_2(t) = -\sum_j \gamma_j {\rm e}^{{\rm i}\varphi_j} B_1(t_j)\Theta(t_j), \tag{12b}$$

where we have defined the phase $\varphi_j = k_{j0}d$ due to the distance between the TLSs, and $\gamma_j = g_{j1}g_{j2}\pi/(v_j\omega_{\rm A})$ are caused by the interaction between the TLSs and the vacuum field in a given transverse mode j, $\Theta(x)$ is the Heaviside unit step function. The decay rate of the l TLS to all ${\rm TM}_j$ modes is denoted by $\Gamma_l = \sum_j \gamma_{lj}$, where $\gamma_{lj} = g_{jl}^2\pi/(v_j\omega_{\rm A})$ is the decay rate of the l-th TLS to the continuum of the ${\rm TM}_j$ mode, the retard effect has been implied by the symbol $t_j = t - \tau_j$. Equations (12a) and (12b) show that the two separate TLSs are coupled after the time $\min\tau_j$ due to the photon emitted by the TLSs travelling in the same modes of the field.

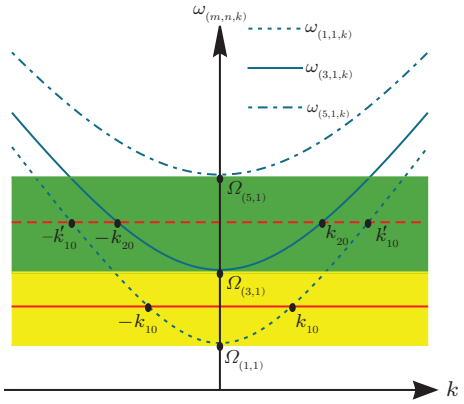


Fig. 2. Dispersion relation of the ${\rm TM}_j$ guiding modes of the waveguide. $\Omega_{(m,n)} = c\sqrt{(m\pi/a)^2 + (n\pi/q)^2}$, $\Omega_{(m,n)}$ is the cutoff frequency. $\omega_{\rm A} \approx (\Omega_{(1,1)} + \Omega_{(3,1)})/2$ (red solid line) and $\omega_{\rm A} \approx (\Omega_{(3,1)} + \Omega_{(5,1)})/2$ (red dashed line). Photons with different frequencies can propagate in different modes with wave numbers $k = k_{10}, k'_{10}, k_{20}, \ldots$.

4. Entanglement dynamics of the TLSs

To measure the amount of the entanglement, we use concurrence as the quantifier.[40] By taking a partial trace over the degrees of freedom of the waveguide, the density matrix of the two TLSs is of an X-form in the two-qubit standard basis $\{|gg\rangle, |eg\rangle, |ge\rangle, |ee\rangle\}$. The concurrence for this type of state can be calculated easily as

$$G(t) = \max(0,\ 2|B_1(t)B_2^*(t)|), \tag{13}$$

for TLSs initially sharing single excitation.

4.1. Single transverse mode

A TLS in its excited state radiates waves into the continua of the modes which are resonant with the TLS. If all TLSs' energy separations lie within the frequency band between $\Omega_{(1,1)}$ and $\Omega_{(3,1)}$ and are far away from the cutoff frequencies $\Omega_{(1,1)}$ and $\Omega_{(3,1)}$, they only emit photons into the ${\rm TM}_{(1,1)}$ $(j=1)$ guiding mode. The equations for the amplitudes of the TLSs read

$$(\partial_t - {\rm i}\xi_1)B_1(t) = -\alpha_1 B_2(t_1)\Theta(t_1), \tag{14a}$$

$$(\partial_t - {\rm i}\xi_2)B_2(t) = -\alpha_1 B_1(t_1)\Theta(t_1), \tag{14b}$$

where $\xi_1 = {\rm i}\gamma_{11} - \delta$, $\xi_2 = {\rm i}\gamma_{21} + \delta$, and $\alpha_1 = \gamma_1 {\rm e}^{{\rm i}\varphi_1}$. By assuming that the TLSs are excited initially and there is no photons in the field, the Laplace transform of Eqs. (14a) and (14b) leads to

$$B_1(s) = \frac{(s-{\rm i}\xi_2)B_1(0) - \alpha_1 {\rm e}^{-s\tau_1}B_2(0)}{(s-{\rm i}\xi_2)(s-{\rm i}\xi_1) - (\alpha_1 {\rm e}^{-s\tau_1})^2}, \tag{15a}$$

$$B_2(s) = \frac{(s-{\rm i}\xi_1)B_2(0) - \alpha_1 {\rm e}^{-s\tau_1}B_1(0)}{(s-{\rm i}\xi_1)(s-{\rm i}\xi_2) - (\alpha_1 {\rm e}^{-s\tau_1})^2}. \tag{15b}$$

The integrand in the inverse Laplace transform yields the time-dependent amplitudes of the TLSs. Defining $t_1^{(n)} = t - n\tau_1$, the integrand can be expanded into a power series

$$\begin{aligned} B_1(t) = {} & \sum_{n=0}^{\infty} B_1(0)\Theta\left(t_1^{(2n)}\right)\left[A_n(\xi_2) + D_n(\xi_1)\right] \\ & - \sum_{n=0}^{\infty} B_2(0)\Theta\left(t_1^{(2n+1)}\right)\left[E_n(\xi_2) + E_n(\xi_1)\right], \end{aligned} \tag{16a}$$

$$\begin{aligned} B_2(t) = {} & \sum_{n=0}^{\infty} B_2(0)\Theta\left(t_1^{(2n)}\right)\left[A_n(\xi_1) + D_n(\xi_2)\right] \\ & - \sum_{n=0}^{\infty} B_1(0)\Theta\left(t_1^{(2n+1)}\right)\left[E_n(\xi_1) + E_n(\xi_2)\right], \end{aligned} \tag{16b}$$

where the functions are defined as

$$A_n(\xi_k) = \lim_{z\to\xi_k} \frac{{\rm d}^{n-1}}{{\rm d}z^{n-1}} \frac{(-{\rm i}\alpha_1)^{2n}\,{\rm e}^{{\rm i}zt_1^{(2n)}}}{(n-1)!\,(z-\xi_l)^{n+1}}, \tag{17a}$$

$$D_n(\xi_k) = \lim_{z\to\xi_k} \frac{{\rm d}^{n}}{{\rm d}z^{n}} \frac{(-{\rm i}\alpha_1)^{2n}\,{\rm e}^{{\rm i}zt_1^{(2n)}}}{n!\,(z-\xi_l)^{n}}, \tag{17b}$$

$$E_n(\xi_k)=\lim_{z\to\xi_k}\frac{\mathrm{d}^n}{\mathrm{d}z^n}\frac{\left(-\mathrm{i}\gamma_1\mathrm{e}^{\mathrm{i}\varphi_1}\right)^{2n+1}\mathrm{e}^{\mathrm{i}zt_1^{(2n+1)}}}{n!\,(z-\xi_l)^{n+1}}. \tag{17c}$$

with subscripts $k,l\in\{1,2\}$ and $k\neq l$. The TLSs show different behaviors depending on the retardation times $n\tau_1$ required for light to travel between two TLSs located at a finite distance, the phase φ_1, the difference δ of the TLSs' frequencies and the difference $\gamma_{11}-\gamma_{21}$ of the decaying factors. For $t\in[0,\tau_1]$, only one term appears

$$B_l(t)=B_l(0)\,\mathrm{e}^{\mathrm{i}\xi_l t}. \tag{18}$$

Two TLSs decays as if they are isolated in the waveguide, so the concurrence decay from $|B_1(0)B_2(0)|$ with a rate $\gamma_{11}+\gamma_{21}$. As long as $(\gamma_{11}+\gamma_{21})\,\tau_1\gg 1$, two TLSs emit photons independently, the photon travels along the waveguide for time τ_1, then the part toward the other TLS will be absorbed, and the TLSs is partially excited, later TLSs re-emit the photon again, the whole process of emission and absorption was repeated as time goes on, however no interference occurs, so the phase φ_1 has no effect on the entanglement. Equation (18) is also the solution of Eq. (14) with $\tau_1\to\infty$. If the TLSs decay slowly so that $(\gamma_{11}+\gamma_{21})\,\tau_1$ is smaller than or equal to 1, it is possible for a TLS to be aware of the other very soon, interference can be produced by multiple re-emissions and re-absorptions of light, which leads to an oscillatory energy exchange between the TLSs. It can be easily seen that the atomic upper state population contains two terms for $t\in[\tau_1,2\tau_1]$

$$B_1(t)=B_1(0)\,\mathrm{e}^{\mathrm{i}\xi_1 t}-B_2(0)\,\alpha_1\frac{\mathrm{e}^{\mathrm{i}\xi_2(t-\tau_1)}-\mathrm{e}^{\mathrm{i}\xi_1(t-\tau_1)}}{\mathrm{i}\,(\xi_2-\xi_1)},$$

$$B_2(t)=B_2(0)\,\mathrm{e}^{\mathrm{i}\xi_2 t}-B_1(0)\,\alpha_1\frac{\mathrm{e}^{\mathrm{i}\xi_2(t-\tau_1)}-\mathrm{e}^{\mathrm{i}\xi_1(t-\tau_1)}}{\mathrm{i}\,(\xi_2-\xi_1)}.$$

The second term in the last equation shows that the TLS is aware of the other, and presents the absorption and re-emission of the other TLS, so interference is possible. As time goes on, multiple re-emissions and re-absorptions of photons appear which implied in the summation in Eq. (16), then the phase φ_1 has the influence on the energy exchange between TLSs. To show the effect of the energy difference δ of the uncoupled state $|eg\rangle$ and $|ge\rangle$ on the entanglement dynamics, we consider the dipoles $\mu_l=\mu$, so the damping rates $\gamma_{11}=\gamma_{12}=\gamma_1$. It is known in Ref. [41] that there is a dark state for two identical TLSs which is completely isolated and evolves independently, it can preserve the concurrence, the dark state could be the symmetry state $|s\rangle=(|eg\rangle+|ge\rangle)/\sqrt{2}$ while the antisymmetry state $|a\rangle=(|eg\rangle-|ge\rangle)/\sqrt{2}$ could have a maximum damping rate 2γ for the phases $\varphi_1=(2n+1)\pi$, $(n=0,1,2,\ldots)$; the antisymmetry state $|a\rangle$ is the dark state while the symmetry state $|s\rangle$ could have a maximum damping rate 2γ for the phase $\varphi_1=2n\pi$. In terms of the amplitudes $C_\mathrm{a}(t)$ and $C_\mathrm{s}(t)$ of the antisymmetry and symmetry states, equation (14) can be written as

$$(\partial_t+\gamma_1)\,C_\mathrm{s}(t)=-\mathrm{i}\delta C_\mathrm{a}(t)-\alpha_1 C_\mathrm{s}(t_1)\,\Theta(t_1), \tag{19a}$$

$$(\partial_t+\gamma_1)\,C_\mathrm{a}(t)=-\mathrm{i}\delta C_\mathrm{s}(t)+\alpha_1 C_\mathrm{a}(t_1)\,\Theta(t_1). \tag{19b}$$

In Fig. 3, we plot the concurrence as a function of the time in unit of τ_1 with the TLSs initially in the antisymmetry state $|a\rangle$ for $\gamma_1\lambda_1/v_1=1.5\times10^{-10}$ where the wavelength $\lambda_1 k_{10}=2\pi$. The evolution of $G(t)$ is profoundly affected by the difference δ, phase φ_1, and delay time τ_1, where φ_1 and τ_1 are introduced by the inter-TLS distance. It can be observed from Fig. 3(a) that the evolution of $G(t)$ is independent of the finite propagating time of the light for the delay time $\tau_1\ll\gamma_1^{-1}$, the two TLSs act collectively. When $\delta=0$ the antisymmetry state $|a\rangle$ is a dark state which preserve the entanglement among the TLSs; as δ increases but still smaller than 2γ, the concurrence decreases monotonous as time increases, as δ is larger than 2γ, the concurrence decreases non-monotonically. The dependence of the entanglement on δ in Fig. 3(a) can be understood by letting $\tau_1\to0$. In this case, equation (19) becomes

$$\partial_t C_\mathrm{s}(t)=-\mathrm{i}\delta C_\mathrm{a}(t)-2\gamma_1 C_\mathrm{s}(t),$$

$$\partial_t C_\mathrm{a}(t)=-\mathrm{i}\delta C_\mathrm{s}(t).$$

As long as $\delta\neq0$, the energy difference δ of two TLSs introduces the coupling between states $|s\rangle$ and $|a\rangle$. The symmetry state $|s\rangle$ is not only coupled to the antisymmetry state $|a\rangle$ but also coupled to the broad continua of the field, the coupling of the state $|s\rangle$ to the field introduces the dissipation, which is characterized by the damping rate 2γ. The energy loss occurs when the $|s\rangle$ is populated. When $2\gamma>\delta$, the loss out of the two TLSs plays an dominant role, the initially occupied state $|a\rangle$ exchanges energy with the state $|s\rangle$, but the energy in the state $|s\rangle$ losses to the field quickly, so it cannot be back to the state $|a\rangle$, this is why the concurrence is a monotonically decreasing function of time. When $2\gamma<\delta$, the population in the state $|s\rangle$ can transfer back to the state $|a\rangle$, so the concurrence undergoes oscillations before decaying to zero. As the inter-TLS separation increases a little bit to meet $\tau_1\sim\gamma_1^{-1}$ as shown in Fig. 3(b), the interference produced by multiple re-emissions and re-absorptions of the photon results in the entanglement oscillating even when $\delta=0$. However, the exchange of the population reduces the magnitude of the concurrence. Panel (c) of Fig. 3 illustrates the dynamics of entanglement for a larger inter-TLS distance with $\tau_1\gg\gamma_1^{-1}$. It can be observed that at time interval $[0,\tau_1]$, each initially excited TLS emits light to the waveguide, and the entanglement

decays exponentially from unity to zero. The radiation field emitted into the waveguide returns to the TLSs after τ_1, then the entanglement is created. But, the periodic maxima of the concurrence are decreased in magnitude as time increases due to the energy loss carried away by the forward-going and the backward-going waves. Population exchange introduced by the energy difference δ further lower the periodic maxima of the concurrence, however, oscillations can be observed when $\delta > 2\gamma$ after time τ_1. We would like to note that non-vanishing δ can also raise the transient behaviors of the concurrence if the TLSs are initially in the symmetry state $|s\rangle$ with $\varphi_1 = 2n\pi$, $(n = 0, 1, 2, \ldots)$, as shown in Fig. 4.

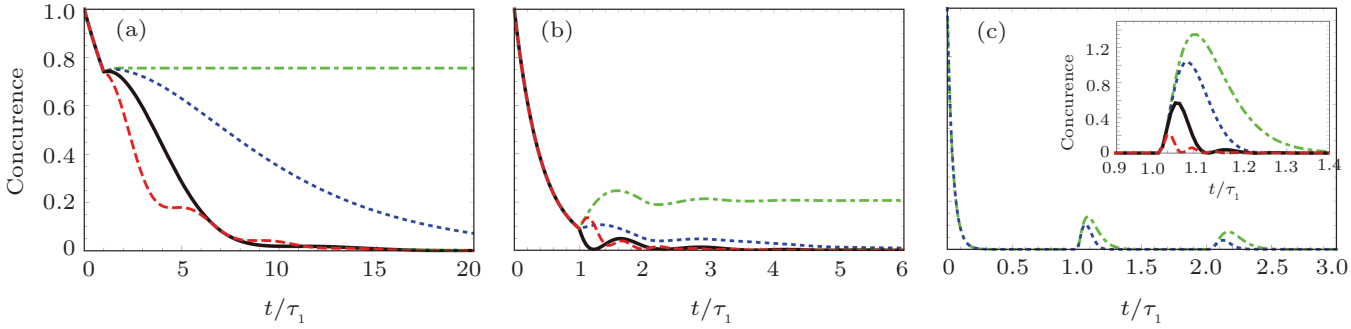


Fig. 3. The concurrence between the TLSs as functions of the dimensionless time t/τ_1 with the TLSs initially in the antisymmetry state $|a\rangle$ for a difference energy separation $\delta = 0$ (green dot-dashed line), $\delta = \gamma$ (blue dotted line), $\delta = 2\gamma$ (black solid line), $\delta = 5\gamma$ (red dashed line) in (a) $\tau_1 v_1/\lambda_1 = 1.0 \times 10^9$, (b) $\tau_1 v_1/\lambda_1 = 8.0 \times 10^9$, (c) $\tau_1 v_1/\lambda_1 = 8.0 \times 10^{10}$. We have set the following parameters: $a = 2q$, $\omega_A = (\Omega_{(1,1)} + \Omega_{(3,1)})/2$, $\gamma_1 \lambda_1/v_1 = 1.5 \times 10^{-10}$, $\varphi_1 = 2\pi\tau_1 v_1/\lambda_1$.

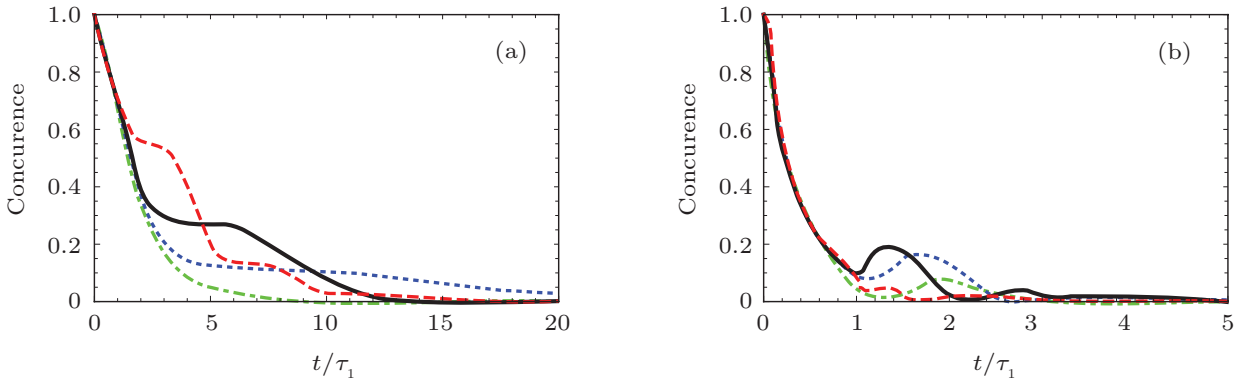


Fig. 4. The concurrence between the TLSs as functions of the dimensionless time t/τ_1 with the TLSs initially in the symmetry state $|s\rangle$ for a difference energy separation $\delta = 0$ (green dot-dashed line), $\delta = \gamma$ (blue dotted line), $\delta = 2\gamma$ (black solid line), $\delta = 5\gamma$ (red dashed line) in (a) $\tau_1 v_1/\lambda_1 = 1.0 \times 10^9$, (b) $\tau_1 v_1/\lambda_1 = 8.0 \times 10^9$. Other parameters are the same as those in Fig. 3.

4.2. Two transverse modes

As the energy splitting of both TLS increases so that they are much larger than the cutoff frequency $\Omega_{(3,1)}$ and much smaller than $\Omega_{(5,1)}$, the TLSs interacts with the field of both $\mathrm{TM}_{(1,1)}$ and $\mathrm{TM}_{(3,1)}$ guiding modes. For dipoles $\mu_l = \mu$, the equations for the amplitudes of the symmetry and antisymmetry states reads

$$\partial_t C_s(t) + \Gamma C_s(t) + \mathrm{i}\delta C_a(t) = -\alpha_1 C_s(t_1)\Theta(t_1) - \alpha_2 C_s(t_2)\Theta(t_2), \tag{20a}$$

$$\partial_t C_a(t) + \Gamma C_a(t) + \mathrm{i}\delta C_s(t) = \alpha_1 C_a(t_1)\Theta(t_1) + \alpha_2 C_a(t_2)\Theta(t_2), \tag{20b}$$

where $\Gamma = \gamma_1 + \gamma_2$ and $\alpha_j = \gamma_j \mathrm{e}^{\mathrm{i}\varphi_j}$ $(j = 1, 2)$. The definitions of delay time τ_j and phase φ_j indicate that $\tau_j < \tau_{j+1}$ and $\varphi_j < \varphi_{j+1}$ for a given TLSs' separation. Through an inspection of Eq. (20) for $d = 0$, it can be found that the antisymmetry state $|a\rangle$ is still a dark state and the symmetry state $|s\rangle$ has a maximum damping rate 2Γ. As d increases a little bit but still satisfying $\varphi_1 = 2n\pi$, $(n = 0, 1, 2, \ldots)$ and the energy difference $\delta = 0$, state $|a\rangle$ is no longer a dark state, it damps with a damping rate $\gamma_2 - \mathrm{Re}\,\alpha_2$, the width of state $|s\rangle$ becomes $2\gamma_1 + \gamma_2 + \mathrm{Re}\,\alpha_2$ which is smaller than 2Γ, but there is a energy splitting $2\,\mathrm{Im}\,\alpha_2$ between the two states. when $\delta \neq 0$, the two states are coupled to each other, so the oscillation strength is changed from $J = \delta$ in one guiding mode to $J = \sqrt{\delta^2 + (\mathrm{Im}\,\alpha_2)^2}$ in two guiding modes, the damping rates

of the two states are also changed. As long as the oscillation strength J is larger than the sum 2Γ, the population will oscillate obviously when the effect of the phase on the dynamics is more important than the delay time.

In Fig. 5, we have plotted the concurrence between the TLSs as a function of the dimensionless time t/τ_1 with the TLSs initially in the antisymmetry state $|a\rangle$. Panel (a) shows the entanglement dynamics when the inter-TLS distance $d = 0$ with different δ, it can be found that the concurrence remain its initial value when $\delta = 0$, however, as δ increases until 2Γ, the faster the population changes between the two states, the faster the concurrence decays. As δ increases further, *i.e.*, more than 2Γ, there is an oscillation. In panel (b), the delay time $\tau_2 \ll \gamma_2^{-1}$, which means there is no delay in the absorption of the energy by another TLS in both $\mathrm{TM}_{(1,1)}$ and $\mathrm{TM}_{(3,1)}$ modes. The antisymmetry state interacts with the field in $\mathrm{TM}_{(3,1)}$ guiding mode due to the phase $\varphi_2 \neq 2n\pi$, the concurrence undergoes an exponential decay when $\delta = 0$. Although the concurrence is further decreased by the increasing of δ, its evolution deviates from the exponential decay. The dotted blue line in panel (c) exhibits a behavior different from that in panel (b), which indicates that phases and delay times play an equal role. In the interval $[0, \tau_2]$, the concurrence exponentially decay with a rate Γ up to time τ_1. After this, it still decreases but deviates from the exponential decay, which means that the phase φ_1 begins to have an effect until time $t = \tau_2$. After time τ_2, the dynamics can be dramatically affected by the phases φ_j, delay times τ_j when $\delta = 0$. However, the energy difference δ can increase the entanglement. We note that in the interval $[0, \tau_1]$, the exponential decay of the concurrence is independent of δ, but it is possible for the population of state $|a\rangle$ to present an oscillating behavior as shown in Fig. 6 since the amplitudes obeys the following equation:

$$\partial_t C_\mathrm{s}(t) + \Gamma C_\mathrm{s}(t) + \mathrm{i}\delta C_\mathrm{a}(t) = 0, \tag{21a}$$

$$\partial_t C_\mathrm{a}(t) + \Gamma C_\mathrm{a}(t) + \mathrm{i}\delta C_\mathrm{s}(t) = 0. \tag{21b}$$

This equation can also explain the exponential decay of panel (d) of Fig. 5 in the time interval $[0, \tau_1]$. Actually, equation (21) also describes the dynamics of TLSs when the delay time $\tau_1 \to \infty$, it indicates that two TLSs emit photons independently, and the emitted photon travels along the waveguide and is never absorbed by the TLSs. For two TLSs far apart as shown in Fig. 5(d), the phase φ_j do not make sense, and the increase of δ lowers the magnitude of the concurrence.Although the emitted photon could be absorbed by the TLS resulting the birth of entanglement, but the revival time becomes $p\tau_1 + q\tau_2$ with p, q are integer, which can be obtained by performing the Laplace transformation on Eq. (12) with $j = 1, 2$.

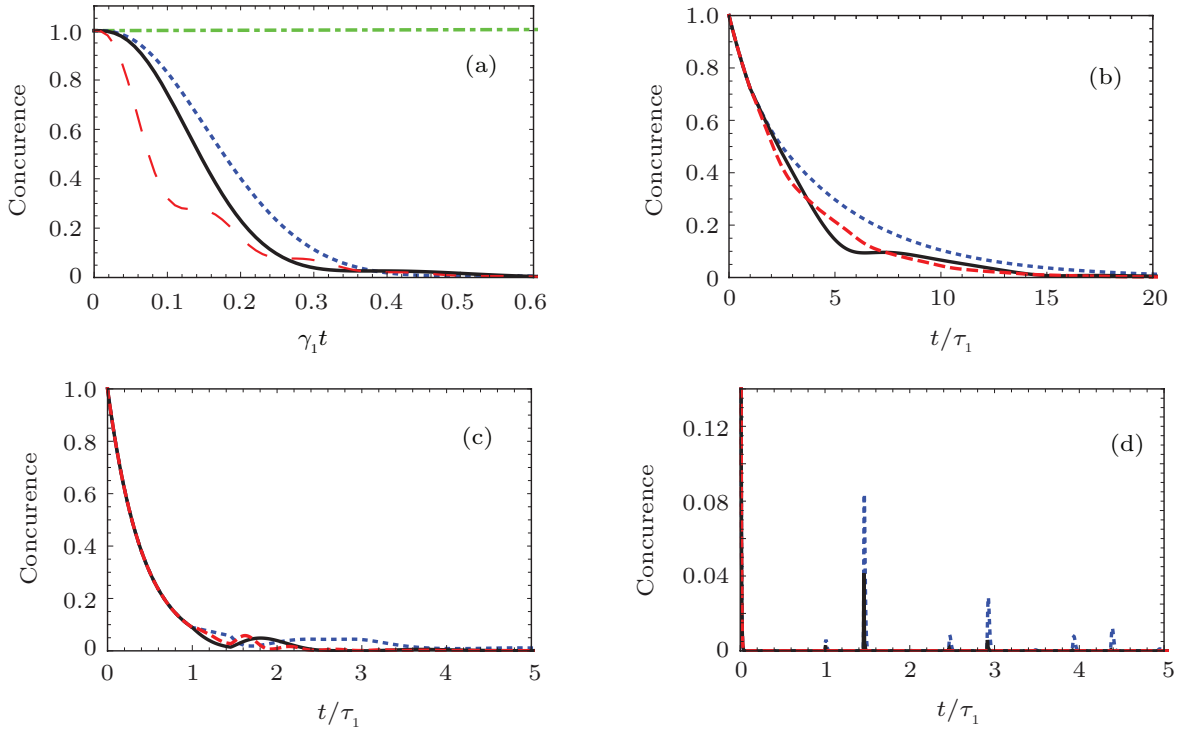


Fig. 5. The concurrence of the TLSs as functions of the dimensionless time t/τ_1 with the TLSs initially in the antisymmetry state $|a\rangle$ and $a = 2q$, $\omega_\mathrm{A} = (\Omega_{(3,1)} + \Omega_{(5,1)})/2$, $\gamma_1\lambda_1/v_1 = 1.1 \times 10^{-11}$, and $\varphi_1 = 2\pi\tau_1 v_1/\lambda_1$. Panel (a): $\tau_1 v_1/\lambda_1 = 0$, $\delta = 0$ for dash–dotted green line, $\delta = 2\gamma_2$ for dotted blue line, $\delta = 2(\gamma_1 + \gamma_2)$ for black solid line, $\delta = 5(\gamma_1 + \gamma_2)$ for dashed red line. In panels (b)–(d), $\delta = 0$ for dotted blue line, $\delta = 1.5\gamma_1 + 2\gamma_2$ for solid black line, $\delta = 5(\gamma_1 + \gamma_2)$ for dashed red line, and the phases are different: $\tau_1 v_1/\lambda_1 = 3.1 \times 10^9$ in panel (b), $\tau_1 v_1/\lambda_1 = 2.3 \times 10^{10}$ in panel (c), $\tau_1 v_1/\lambda_1 = 1.8 \times 10^{12}$ in panel (d).

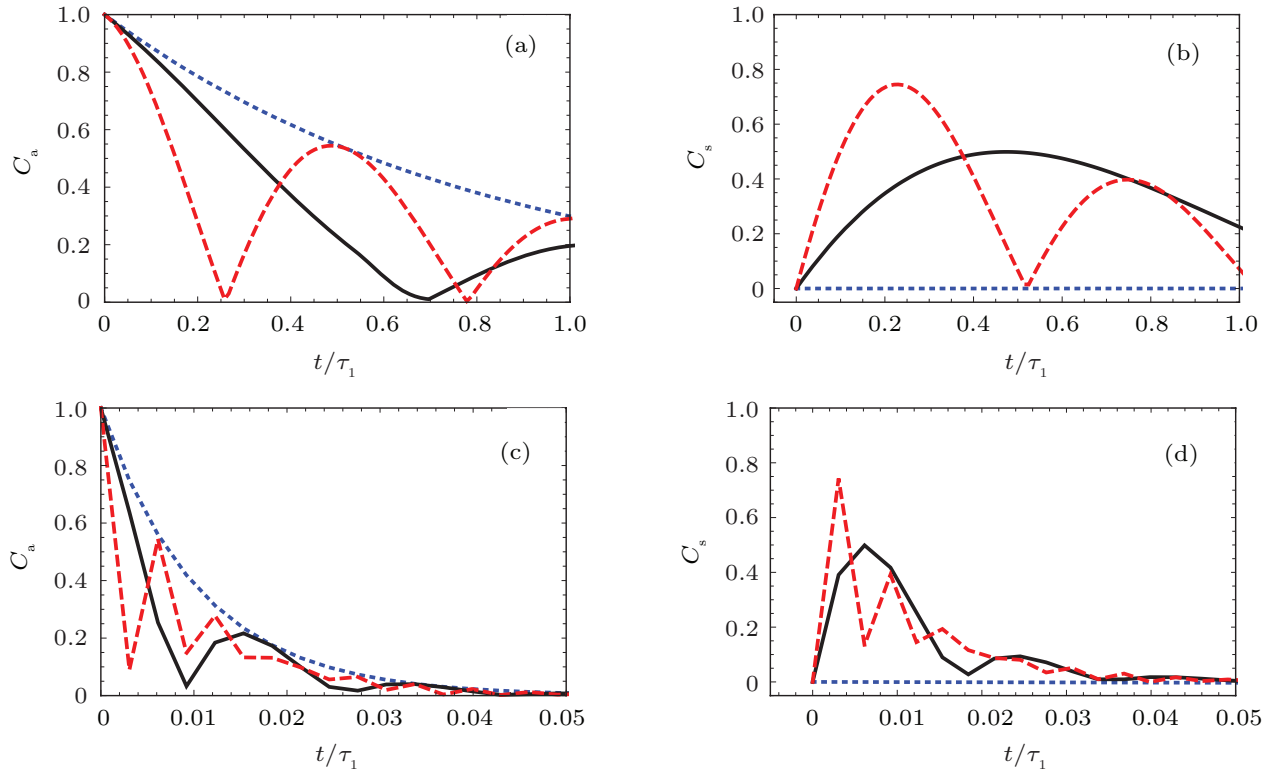


Fig. 6. The populations of the symmetry and antisymmetry states in the time interval $[0, \tau_1]$ of Figs. 5(c) and 5(d). Here, $\delta = 0$ for dotted blue line, $\delta = 1.5\gamma_1 + 2\gamma_2$ for solid black line, $\delta = 5(\gamma_1 + \gamma_2)$ for dashed red line, and $\varphi_1 = 2\pi\tau_1 v_1/\lambda_1$; $\tau_1 v_1/\lambda_1 = 2.3 \times 10^{10}$ in panels (a) and (b), $\tau_1 v_1/\lambda_1 = 1.8 \times 10^{12}$ in panels (c) and (d).

5. Conclusion

We have studied two TLSs coupled to the vacuum of guiding modes confined in a rectangular waveguide. Two TLSs are fixed at different points in the waveguide and initially share an excitation. For the energy separation of the TLSs far away from the cutoff frequencies of transverse modes, two coupled delay-differential equations are obtained for the probability amplitudes of the TLSs. The inter-TLS distance induces phase factors and delay times in the delay differential equations. The energy difference introduces the coupling between the symmetry and antisymmetry state. For the inter-TLS distance $d = 0$, the entanglement can be trapped in the antisymmetry state when $\delta = 0$ since the antisymmetry state is decoupled with the guiding mode, however, the non-vanishing δ prevents entanglement from being trapped. As d increases to satisfy $\max\{\tau_j\} \ll \gamma_j^{-1}$, two TLSs behave collectively. It is well known that a change of phase leads to an enhanced or inhibited exponential decay of the concurrence, however, δ makes the dynamics of the concurrence deviating from the exponential decay. As d increases further so that $\max\{\tau_j\} \approx \gamma_j^{-1}$, although the interference produced by multiple reemissions and reabsorptions of photon results in the dynamic behavior of the entanglement deviating from the exponential decay, non-zero δ can raise the entanglement in transient as time increases. When $\tau_j \gg \gamma_j^{-1}$, an increasing of δ only lowers the entanglement.

References

[1] Kimble H J 2008 *Nature* **453** 1023
[2] Dicke R H 1954 *Phys. Rev.* **93** 99
[3] Lehmberg R H 1970 *Phys. Rev. A* **2** 883
[4] Milonni P W and Knight P L 1974 *Phys. Rev. A* **10** 1096
[5] Milonni P W and Knight P L 1975 *Phys. Rev. A* **11** 1090
[6] Cook R J and Milonni P W 1987 *Phys. Rev. A* **35** 5081
[7] Yu T and Eberly J H 2004 *Phys. Rev. Lett.* **93** 140404
[8] Yu T and Eberly J H 2006 *Phys. Rev. Lett.* **97** 140403
[9] Ficek Z and Tanas R 2006 *Phys. Rev. A* **74** 024304
[10] Ficek Z and Tanas R 2008 *Phys. Rev. A* **77** 054301
[11] Zhou L, Yang L P, Li Y and Sun C P 2013 *Phys. Rev. Lett.* **111** 103604
[12] Lu J, Zhou L, Kuang L M and Nori F 2014 *Phys. Rev. A* **89** 013805
[13] Lu J, Wang Z H and Zhou L 2015 *Opt. Express.* **23** 22955
[14] Shen J T and Fan S 2005 *Phys. Rev. Lett.* **95** 213001
[15] Shen J T and Fan S 2005 *Opt. Lett.* **30** 2001
[16] Shen J T and Fan S 2007 *Phys. Rev. Lett.* **98** 153003
[17] Zhou L, Gong Z R, Liu Y X, Sun C P and Nori F 2008 *Phys. Rev. Lett.* **101** 100501
[18] Dong H, Gong Z R, Ian H, Zhou L and Sun C P 2009 *Phys. Rev. A* **79** 063847
[19] Zheng H X, D Gauthier J and Baranger H U 2010 *Phys. Rev. A* **82** 063816
[20] Zheng H X, D Gauthier J and Baranger H U 2011 *Phys. Rev. Lett.* **107** 223601
[21] Zheng H X, D Gauthier J and Baranger H U 2012 *Phys. Rev. A* **85** 043832
[22] Zheng H X, D Gauthier J and Baranger H U 2013 *Phys. Rev. Lett.* **111** 090502

[23] Tsoi T S and Law C K 2008 *Phys. Rev. A* **78** 063832
[24] Shi T and Sun C P 2009 *Phys. Rev. B* **79** 205111
[25] Shi T, Fan S and Sun C P 2011 *Phys. Rev. A* **84** 063803
[26] Shi T and Fan S 2013 *Phys. Rev. A* **87** 063818
[27] Laakso M and Pletyukhov M 2014 *Phys. Rev. Lett.* **113** 183601
[28] Redchenko E S and Yudson V I 2014 *Phys. Rev. A* **90** 063829
[29] Ordonez G and Kim Sungyun 2004 *Phys. Rev. A* **70** 032702
[30] Fang Y L L and Baranger H U 2015 *Phys. Rev. A* **91** 053845
[31] Roy D, Wilson C M and Firstenberg O 2017 *Rev. Mod. Phys.* **89** 021001
[32] Sinha K, Meystre P, Goldschmidt E A, Fatemi F K, Rolston S L and Solano P 2020 *Phys. Rev. Lett.* **124** 043603
[33] Sinha K, Gonz A, Yong L and Pablo S 2020 *Phys. Rev. A.* **102** 043718
[34] Kong J A 1986 *Electromagnetic Wave Theory* (New York: John Wiley and Sons) p. 135
[35] Dung H T and Ujihara K 1999 *Phys. Rev. A* **59** 2524
[36] Dorner U and Zoller P 2002 *Phys. Rev. A* **66** 023816
[37] Rist S, Eschner J, Hennrich M and Morigi G 2008 *Phys. Rev. A* **78** 013808
[38] Gulfam Q A, Ficek Z and Evers J 2012 *Phys. Rev. A* **86** 022325
[39] Lu J, Zhou L and Fu H C 2013 *Phys. Lett. A* **377** 1255
[40] Wootters William K 1998 *Phys. Rev. Lett.* **80** 2245
[41] Hu L, Lu G, Lu J and Zhou L 2020 *Quantum Inf. Process.* **19** 81